wjert, 2020, Vol. 6, Issue 2, 583-595. *Original Article* ISSN 2454-695X

World Journal of Engineering Research and Technology

WJERT

www.wjert.org SJIF Impact Factor: 5.924

INFLUENCE OF METAL DIBORIDE AND SUPERCONDUCTIVITY IN TELLIRIUM BASED COMPOUND TeB_2: A FIRST PRINCIPLE STUDY

Ashwani Kumar*

Faculty of Sciences (Physics), National Defence Academy, Khadakwasla, Pune – 411 023.

Article Received on 20/02/2020 **Article Revised on 10/03/2020** **Article Accepted on 30/03/2020**

***Corresponding Author**
Ashwani Kumar
Faculty of Sciences (Physics), National Defence Academy, Khadakwasla, Pune – 411 023.

ABSTRACT

An attempt has been made in the present manuscript to study the concentration dependent study of various superconducting state parameters. In this paper, the superconducting state parameters like Coulomb pseudopotential μ^*, electron – phonon coupling strength λ, SC transition temperature T_C, interaction strength N_OV, semi band gap Δ, energy or mass renormalization parameter Z_0 and isotope effect exponent δ have been studied to explore their dependency on concentration. Harrison's First Principle pseudopotential (HFPP) method is applied in conjunction with BCS theory and McMillan's formalism has been used in order to understand the present investigation.

KEYWORDS: BCS theory, Superconductivity, Diboride, Pseudopotential.

1. INTRODUCTION

The monolayer superconductors (MSC), in two dimensional (2-D) limits provides well defined platform for superconductivity (SC) study.[1-5] The discovery of high transition temperature in monolayer superconductivity makes them potential candidate for high temperature superconductivity.[6-7] But due to presence of interface bonds in monolayer superconductivity, the occurrence of superconductivity is limited to only certain substrates.[6-8] Moreover, the growth of monolayer superconductivity is limited to occur only under ultra high vacuum in order to minimize substrate induced defects,[9] In light of complexity involved in development of superconductivity in other materials, the boride based materials sparked interest in such materials.[10-12] This class of material is promising candidates for superconducting cables in order to fulfill future energy demands because these materials can

easily be fabricated into wires for high current applications. Although these materials has been studied by several researcher in the past in context with various factors like temperature dependence, pressure dependence etc.[13-21] but the study of concentration dependence and its impact on various parameters are still unexplored.

In the present paper, an attempt has been made to study the effect of concentration dependence on superconducting parameter in TeB_2 material for the first time in conjunction with BCS theory. The BCS theory can safely be applied to this class of material.[22] The pseudopotential formalism in conjunction with Faber – Ziman formalism has also been applied for computation of form factor and consequently the Mc Millan's formalism is employed for the computation of superconducting state transition temperature. The SC properties like Coulomb pseudopotential μ^*, electron – phonon coupling strength λ, SC state transition temperature T_C, the mass or energy renormalization parameter Z_0, the effective interaction strength N(0)V, the isotope effect exponent δ are calculated.

2. Formalism and Computation

2.1 Form Factor

Form Factor is the Fourier transform of the crystal potential in the reciprocal lattice. It is the potential dependent term and algebraic sum of interacting potentials. The interacting potentials are

1. Effective valence charge and core electron potential, v_{ab}^*
2. Effective conduction band core exchange potential, v_c^*
3. Effective conduction electron potential, v_d^*
4. Effective screening potential, v_f^*
5. Repulsive potential, W^R

These interacting potentials are further classified as

a) Energy dependent components like

Repulsive potential W^R: It is the only repulsive component of the form factor and it comprises the core energy eigenvalues and can be expressed as:

$$W^R = \langle \mathbf{k}+\mathbf{q} | W^R | \mathbf{k} \rangle$$

$$\Rightarrow W^R = \sum_{nl} \left(k^2 + f_{nl}\right)(2l+1)\langle \mathbf{k}+\mathbf{q} | nlo \rangle \langle \mathbf{k} | nlo \rangle P_l(Cos\theta)$$

$$+\frac{\sum_{nl}\left(k^2+f_{nl}\right)(2l+1)\langle \mathbf{k}|nlo\rangle^2}{1-\sum_{nl}(2l+1)\langle \mathbf{k}|nlo\rangle^2}\times\frac{\sum_{nl}\left(k^2+f_{nl}\right)(2l+1)\langle \mathbf{k}|nlo\rangle^2}{1-\sum_{nl}(2l+1)\langle \mathbf{k}|nlo\rangle^2}$$

$$\times\left[\sum_{nl}(2l+1)\langle \mathbf{k}+\mathbf{q}|nlo\rangle\langle \mathbf{k}|nlo\rangle P_l(Cos\theta)\right] \quad (1)$$

Where,

$$f_{nl}=-3.6\,Z^*/r_0+v_0^b+v_0^c+|\varepsilon_{nl}|-V_{OPW}$$

Is the core shift that represents the shift in the Hartree energies due to various interacting potentials. Here, the symbol '*o*' with *nl* stands for magnetic quantum number m = 0.

$$\langle \mathbf{k}|\mathbf{nlo}\rangle=\left(\frac{4\pi}{\Omega_0}\right)^{1/2}\int rP_{nl}(r)j_l(kr)dr$$

$$\langle \mathbf{k}+\mathbf{q}|\mathbf{nlo}\rangle=\left(\frac{4\pi}{\Omega_0}\right)^{1/2}\int rP_{nl}(r)j_l(|\mathbf{k}+\mathbf{q}|r)dr$$

Screening potential v_q^f is the interaction between the conduction electrons among themselves and is responsible for the screening of the form factor and is expressed as

$$v_q^f=\frac{4}{\pi k_F\eta^3}\int_{-1}^{+1}\frac{dZ}{\eta+2Z}\int_0^{(1-Z^2)^{1/2}}d\rho 2\rho\langle \mathbf{k}+\mathbf{q}|W^R|\mathbf{k}\rangle \quad (2)$$

b) Energy independent components (which do not involve core energy eigenvalues ε_{nl}) like valence charge and core electron potential, $v_q^{a,b}$, the conduction band core exchange potential, v_q^c, the single OPW conduction electron potential, v_q^d Which when considered together are termed as *bare ionic potential* v_q^0. It consists of the following:

(i) The valence charge potential is the potential arising from the net core charge equal to the valency of the metal and is simply $-Ze^2/r$ where *Z* is the valency and *e* is the electronic charge. It is expressed as

$$v_q^a=-\frac{8\pi Z}{\Omega_0 q^2} \quad (3)$$

(ii) The core potential is the coulomb potential arising from the remainder of the nuclear and expressed as

$$v_q^b = -\frac{8\pi Z}{\Omega_0 q^2}\left[n(r) - n(0)\right] \tag{4}$$

Where,

N(r) = core electron density = $\frac{\sum_{nl} 2(2l+1)P_{nl}^2(r)}{4\pi r^2}$

N(0) = number of core electrons = $\sum_{nl} 2(2l+1)$

The $P_{nl}(r)$ is the normalized radial wave function; n and l are the total and angular quantum numbers respectively when considered together they form a neutral core and thus the potential is localized to the core region. They are termed as valence charge and core electron potential v_q^{ab}.

$$\therefore v_q^{ab} = v_q^a + v_q^b = -\frac{8\pi Z}{\Omega_0 q^2}\left[-Z - n(0) - n(r)\right] \tag{5}$$

(iii) The conduction band core exchange potential is the exchange interaction between the core and conduction electrons. It is included through the Slater's Xα-exchange and can be expressed as:

$$v_q^c = -6\alpha\left(\frac{3}{8\pi}\right)^{1/3}\left(\frac{4\pi}{\Omega_0 q}\right)\int(\sin qr)(r(U(r)))^{1/3}dr \tag{6}$$

Where, α is the conduction band core exchange parameter.

(iv) The conduction electron potential is defined as the potential due to charge density of the single and unnormalized OPW states. Due to the normalization, the probability density gives rise to an orthogonalization hole electron density. The orthogonalization hole assumed to be distributed as the charge as the charge of core electron and is expressed as

$$v_q^d = -\frac{8\pi Z}{\Omega_0 q^2}\frac{n(r)}{n(0)}\left(\frac{Z^*}{Z} - 1\right) \tag{7}$$

Based on this, the energy independent components which are the algebraic sum of the Fourier transform of the above mentioned potential can be obtained as:

$$N\langle \mathbf{k}+\mathbf{q}|V(r)|\mathbf{k}\rangle = v_q^{ab} + v_q^c + v_q^d = v_q^0 \tag{8}$$

This is also known as the Bare – ionic potential.

The non-local screened form factor may be expressed as,

$$w(\mathbf{k},\mathbf{q}) = v_{ab}^{*} + v_{c}^{*} + v_{d}^{*} + v_{f}^{*} + W^{R}$$

$$= v_{0}^{*} + v_{f}^{*} + W^{R} \qquad (9)$$

where, $v_{0}^{*} = v_{ab}^{*} + v_{c}^{*} + v_{d}^{*}$

$$v_{ab}^{*} = \frac{v_{q}^{ab}}{\varepsilon^{*}(q)}; \quad v_{c}^{*} = \frac{v_{q}^{c}}{\varepsilon^{*}(q)}; \; v_{d}^{*} = \frac{v_{q}^{d}}{\varepsilon^{*}(q)}; \; v_{f}^{*} = \frac{v_{q}^{f}}{\varepsilon^{*}(q)}$$

And $W^{R} = \langle \mathbf{k}+\mathbf{q} | W^{R} | \mathbf{k} \rangle$

Due to the contribution of valence electrons, the bare-ionic potential $w^{0}(k,q)$ gets modified. This process is termed as screening of the form-factor and it arises from the exchange-correlation motion of electron being accommodated through exchange-correlation function G(q) or G(η). There are various exchange and correlation functions $\varepsilon^{*}(q)$ like Hubbard – Sham (H-S),[23] Kleinmann – Langreth (K-L),[24] and Shaw,[25] form of screening used by many researchers. The V-S exchange,[22] satisfies the compressibility sum rule. According to the theory given by Vashishta – Singwi,[22] based on research of Singwi *et al.*[26,27] the change in the pair correlation function is incorporated. In case of metallic densities, the self consistent value of G(η) is expressed as

$$G(\eta) = A\left(1 - e^{-B\eta^{2}}\right) \qquad (10)$$

Which is valid only for $\eta \le 2$ where $\eta = q/k_{F}$, the constants A and B satisfies the compressibility rule and are dependent on the Wigner – Seitz sphere radius.

The pseudopotential form factor and other parameters of the binary system may be calculated based on Vegard's law as,

$$X_{AB} = (1-c)X_{A} + cX_{B} \qquad (11)$$

Where, X_A and X_B are the parameters or form factor of the constituents and X_{AB} those of the binary system, c is the concentration of the second constituent.[28]

The Debye temperature (θ_D) of the binary system can be expressed as.[29]

$$\frac{1}{(\theta_{D})_{AB}^{2}} = \frac{1-c}{(\theta_{D})_{A}^{2}} + \frac{c}{(\theta_{D})_{B}^{2}} \qquad (12)$$

The SC parameters can be calculated through the well established McMillan's formalism.[30] The electron – phonon coupling strength is given by

$$\lambda = \frac{12m^* Z^*}{M\langle \omega^2 \rangle} \int_0^1 \eta^3 |w(\mathbf{k},\mathbf{q})|^2 d\eta \tag{13}$$

where m* is the effective mass of the electron, Z* the effective valence, M the atomic mass, $\langle \omega^2 \rangle$ the averaged phonon frequency and $\eta = q/2k_F$.

The Coulomb pseudopotential is represented by

$$\mu^* = \left[\frac{m_b}{\pi k_F}\right] I \Bigg/ \left[1 + \frac{m_b}{(\pi k_F)} \ln\left(\frac{E_F}{K_B \theta_D}\right) I\right] \tag{14}$$

with $I = \int_0^1 \frac{d\eta}{\eta \varepsilon^*(\eta)}$ (15)

Here, m_b is the band mass, E_F the Fermi energy, K_B the Boltzmann constant, θ_D the Debye temperature and k_F the Fermi wave vector. The Superconducting transition temperature is given by

$$T_C = \frac{\theta_D}{1.45} \exp\left\{\frac{-1.04(1+\lambda)}{(\lambda - \mu^*(1+0.62\lambda))}\right\} \tag{16}$$

The energy renormalization parameter is given by

$$Z_0 = \left[1 + \frac{10}{11}\lambda\right] \tag{17}$$

The effective interaction strength is given by

$$N(0)V = \frac{[\lambda - \mu^*]}{1 + \frac{10}{11}\lambda} \tag{18}$$

The isotope effect exponent is given by

$$\delta = \frac{1}{2}\left[1 - \left\{\mu^* \ln\left(\frac{\theta_D}{1.45 T_C}\right)\right\}^2 \frac{1+0.62\lambda}{1.04(1+\lambda)}\right] \tag{19}$$

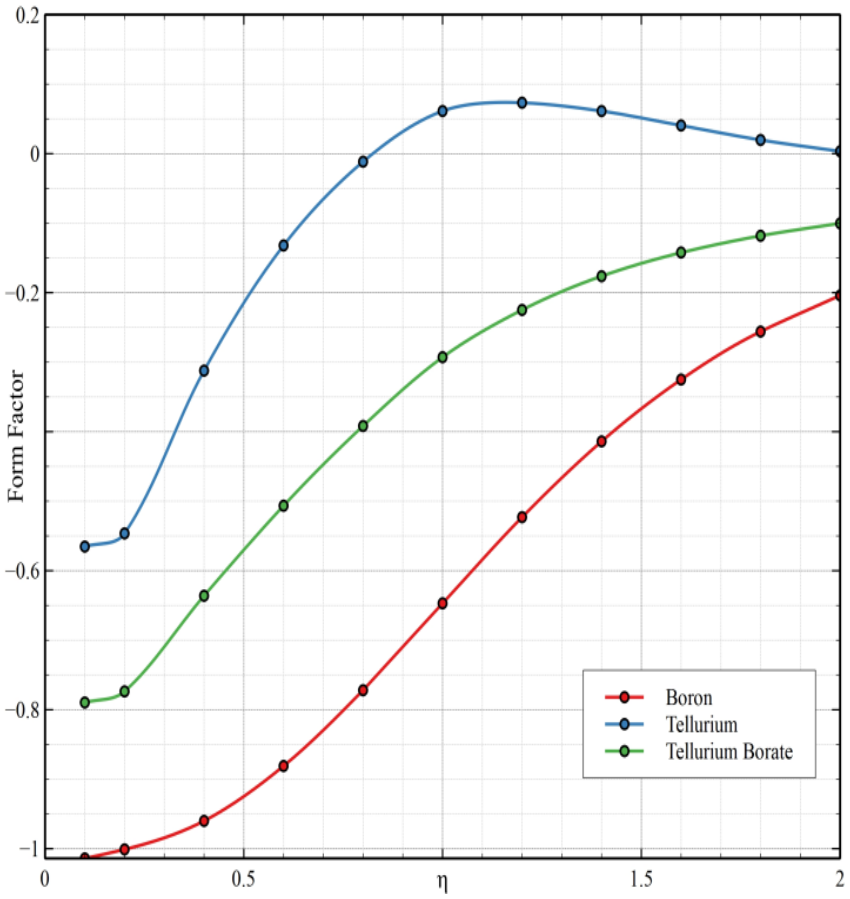
Form Factor
η
Boron
Tellurium
Tellurium Borate

Fig. 1:

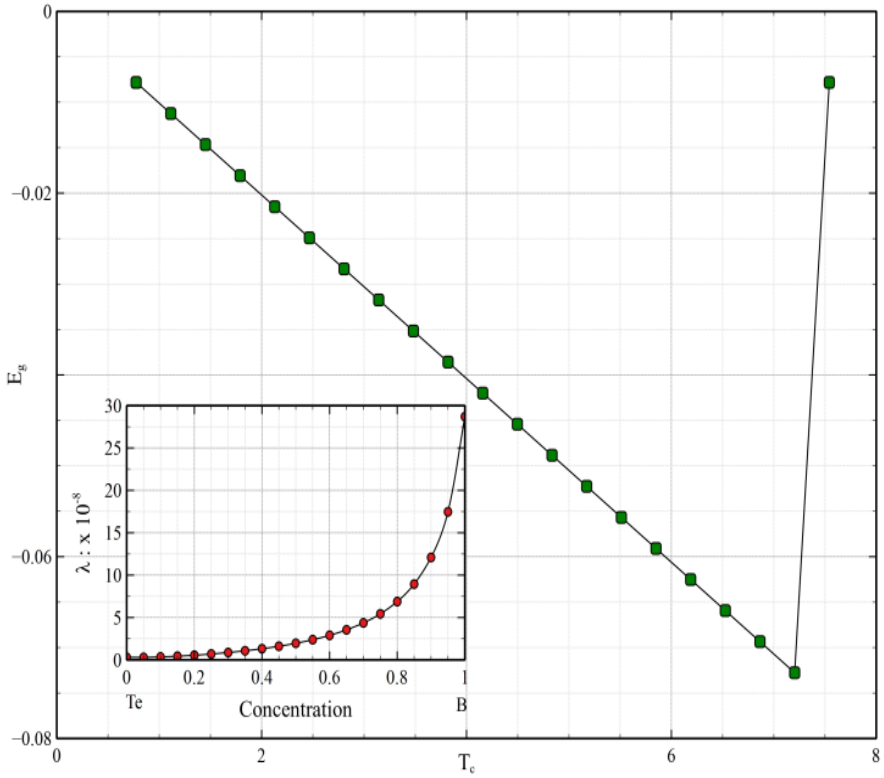
E_g
T_c
λ : x 10⁻⁸
Concentration
Te
B

Fig. 2:

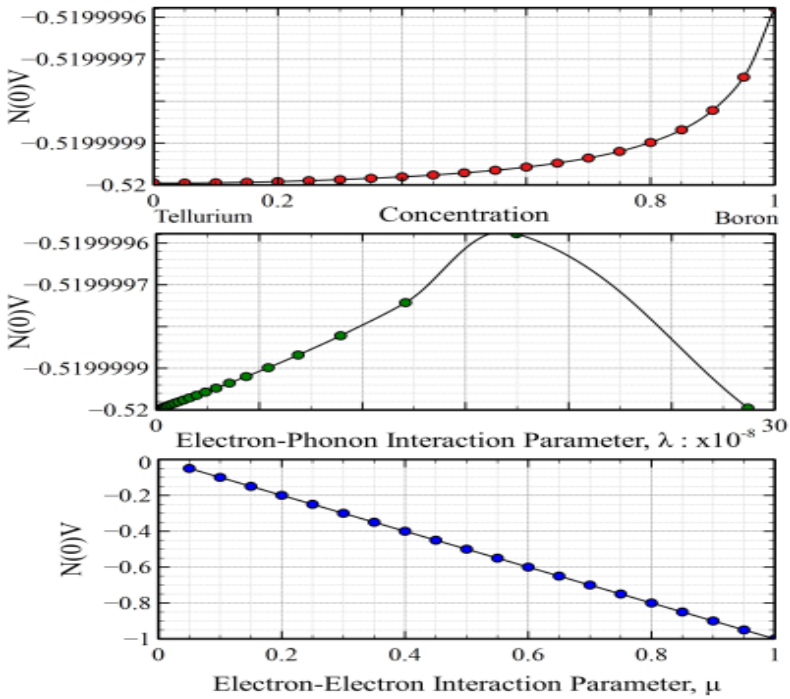
N(0)V
−0.5199996
−0.5199997
−0.5199999
−0.52
0
0.2
0.8
1
Tellurium
Concentration
Boron
Electron-Phonon Interaction Parameter, λ : x10^-8
30
0
−0.2
−0.4
−0.6
−0.8
−1
0.4
0.6
Electron-Electron Interaction Parameter, μ

Fig. 3:

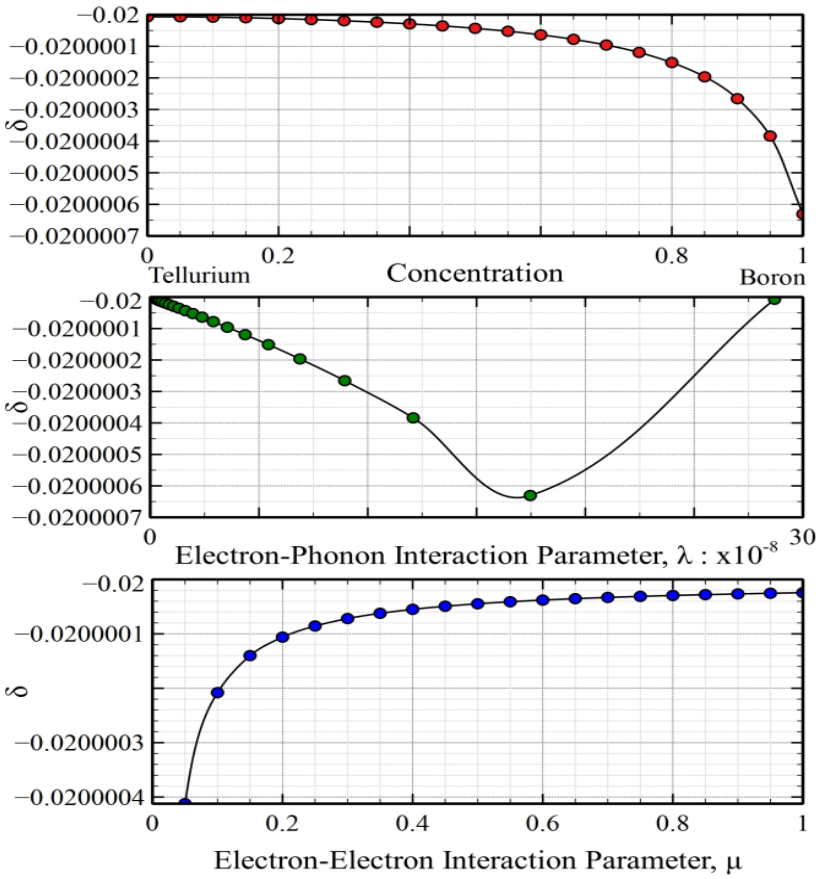
δ
−0.02
−0.0200001
−0.0200002
−0.0200003
−0.0200004
−0.0200005
−0.0200006
−0.0200007
0
0.2
0.8
1
Tellurium
Concentration
Boron
Electron-Phonon Interaction Parameter, λ : x10^-8
30
0.4
0.6
Electron-Electron Interaction Parameter, μ

Fig. 4

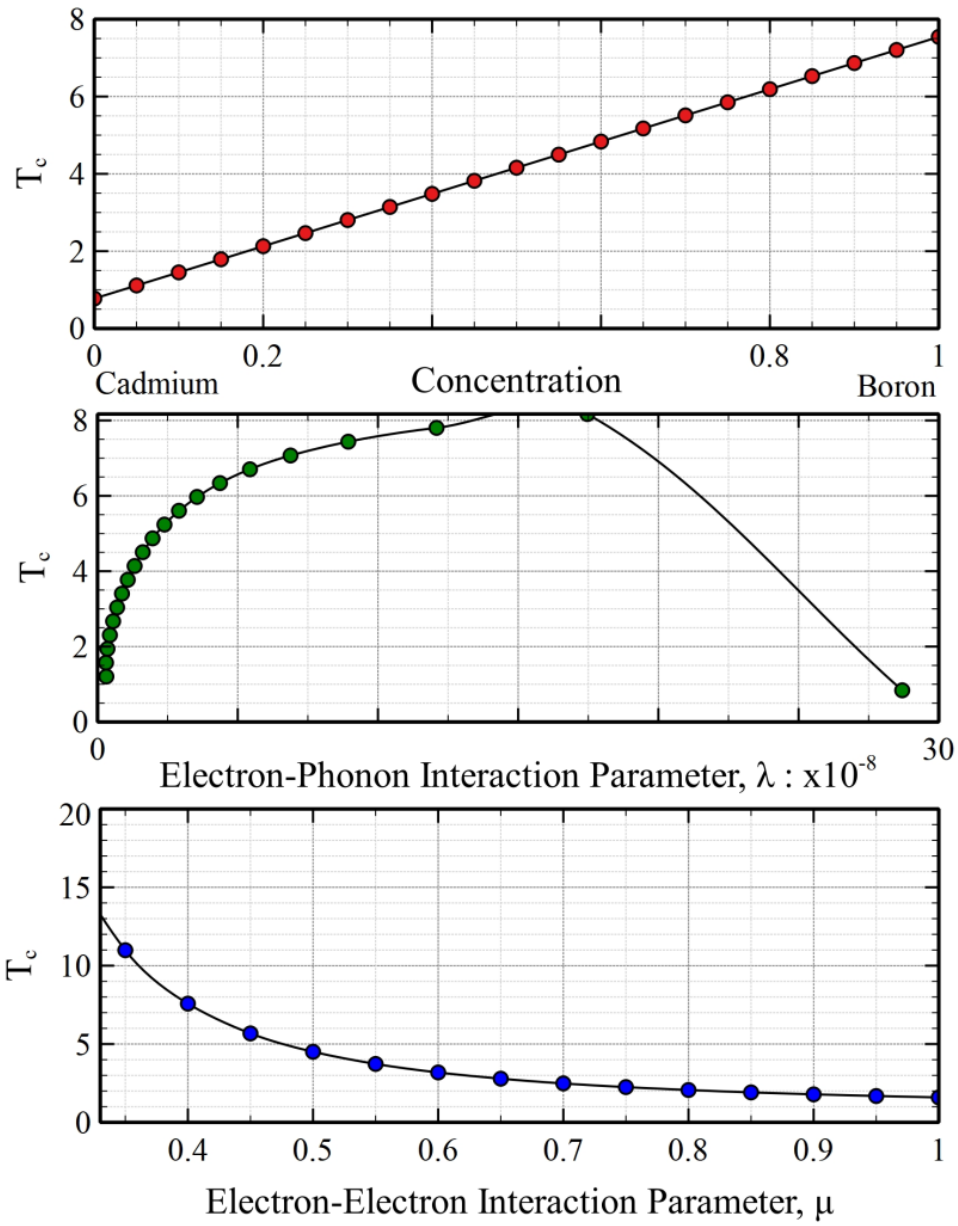

Fig. 5:

3. RESULTS AND DISCUSSION

The calculated form factor w(**k**,**q**) of TeB_2 is presented in **Fig. 1**. It is evident that Te atom dominates the form factor of the compound and hence it plays significant role in calculation of electron – phonon coupling strength and the superconducting transition temperature. The pairing mechanism leading to superconductivity is of phononic region. The most contributing factor is in the region $1 \leq \eta \leq 2$.

In **Fig. 2**, the value of energy gap decreases and almost vanishes around critical temperature of 7 K. The value of energy gap increases suddenly beyond critical temperature. In **Fig. 2 (Inset)**, The value of electron – phonon coupling strength shows quadratic behavior with 2nd order polynomial relationship with the concentration gradient of elements. It increases with the increase in concentration of Boron thereby reflecting gradual transition from weak coupling behavior to intermediate coupling behavior. The same may be attributed to an increase of the hybridization of sp-d electron of Boron with increasing concentration of Boron.

In **Fig. 3**, the magnitude of effective interaction strength signifies that it is a weak coupling superconductor. The value of effective interaction strength shows a quadratic behavior with 2nd order polynomial relationship with concentration. Its magnitude increases with the increase in the value electron phonon coupling strength. It attains a maximum value showing formation of stable superconducting phase whereas its magnitude falls linearly with the increase in the magnitude of coulomb pseudopotential.

In **Fig. 4**, the isotope effect exponent follows parabolic fall with the increase in concentration of Boron. The computed values show a strong dependence on the dielectric screening. It attains a minimum indicating the formation of potential well and hence stable superconducting phases as electron – phonon coupling parameter is varied. Moreover, the isotope effect exponent saturates with the increase in electron – electron interaction parameter.

In **Fig. 5**, the magnitude of critical temperature increases with the concentration of Boron and the same can be well described by linear regression of the data. This behavior can be effectively used for cryogenic applications. It is found that its magnitude increase linearly with the increasing value of electron – phonon coupling strength and attains its maximum around 17×10^{-8}. A further increase in the magnitude of electron phonon coupling strength lead to sharp fall in the magnitude of critical temperature. Similarly, the magnitude of critical temperature falls sharply with the increase in the magnitude of coulomb pseudoptential.

Evaluation of λ through electronic specific heat coefficient γ is given as

$$\lambda = \gamma_{exp.} / \gamma_{calc.} - 1 \qquad (20)$$

Where, $\lambda_{calc.} = 1 / 3\, \pi^2\, D\,(E_F)\, k_B^2$ (21)

The suitable form factors w(k,q) have been identified and they have been used to compute other SC state parameter viz, mass or energy renormalization parameter Z_0, effective interaction strength N(0)V and the isotope effect exponent δ.

The band gap E_g=2 Δ(0) has been calculated as

$$\Delta(0) = \frac{k_B \theta_D}{\text{Sin h}\left[\frac{1}{N(0)V}\right]} \tag{22}$$

where

$$\frac{1}{N(0)V} = \ln \frac{1.14\theta_D}{T_C} \tag{23}$$

It is found that value of energy gap decreases (**Fig. 4, Fig. 5)** and almost vanishes at superconducting Tc. It is observed that the net electron-electron becomes attractive and all electrons are coupled to form cooper pairs in the ground state. The paired electrons are repeatedly scattered between single electron state.

Thus λ and T_C (**Fig. 6)** computed through form factors using various input parameters have also satisfactorily reproduced the other SC state parameters Z_0, N_0V and the band gap Δ.

4. CONCLUSION

The HFPP technique has been successfully implemented in conjunction with BCS theory to study the various properties of TeB_2 inherent in the superconducting state. It is found that B – atoms in the boron layers play more significant role as observed by Singh[30] through band structure calculations. Moreover, TeB_2 crystallizes in hp-3 structure where B – atoms form honeycomb lattice consisting of graphite like sheets separated by hexagonal layers of Al atoms.It is observed that the most contributing part of the form factor w(**k**,**q**) due to Boron atoms in the region 1 ≤η≤ 2 where η = q / k_F. Higher value of T_c can be obtained at low values of μ*. It is found that the electron-phonon coupling parameter, λ behaves quadratically with second order polynomial relationship with the concentration gradient of the elements Al and B forming the alloy TeB_2.The energy gap decreases and almost vanishes at superconducting T_c. It is observed that the net electron-electron becomes attractive and all electrons are coupled to form cooper pairs in the ground state. The pairing mechanism leading to SC is of phononic origin.

Superconducting Parameter of the superconductor TeB_2 having double layered structure where boron atoms form honeycomb lattice separated by hexagonal layers of Al atoms. Superconductivity mainly arises due to Boron. There is a flat band in the vicinity of the Fermi level and the B atoms are involved in electron-phonon coupling in the system.

REFERENCES

1. Saito, Y., Nojima, T. & Iwasa, Y. Highly crystalline 2D superconductors. Nat. Rev. Mater, 2016; 2: 16094.
2. Qin, S., Kim, J., Niu, Q. & Shih, C.-K. Superconductivity at the two-dimensional limit. Science, 2009; 324: 1314–1317.
3. Ugeda, M. M. et al. Characterization of collective ground states in single-layer NbSe2. Nat. Phys, 2016; 12: 92–97.
4. Xi, X. et al. Strongly enhanced charge-density-wave order in monolayer $NbSe_2$. Nat. Nano, 2015; 10: 765–769.
5. Saito, Y., Kasahara, Y., Ye, J., Iwasa, Y. & Nojima, T. Metallic ground state in an ion-gated two-dimensional superconductor. Science, 2015; 350: 409–413.
6. Ge, J.-F. et al. Superconductivity above 100 K in single-layer FeSe films on doped $SrTiO_3$. Nat. Mater, 2015; 14: 285–289.
7. Tan, S. et al. Interface-induced superconductivity and strain-dependent spin density waves in FeSe/$SrTiO_3$ thin films. Nat. Mater., 2013; 12: 634–640.
8. Zhang, T. et al. Superconductivity in one-atomic-layer metal films grown on Si (111). Nat. Phys., 2010; 6: 104–108.
9. Hong Wang, Xiangwei Huang, Junhao Lin, Jian Cui, Yu Chen, Chao Zhu, Fucai Liu, Qingsheng Zeng, Jiadong Zhou, Peng Yu, Xuewen Wang, Haiyong He, Siu Hon Tsang, Weibo Gao, Kazu Suenaga, Fengcai Ma, Changli Yang, Li Lu, Ting Yu, Edwin Hang Tong Teo, Guangtong Liu & Zheng Liu, High-quality monolayer superconductor $NbSe_2$ grown by chemical vapour deposition, Nat. Commn, 2017; 8: 394. DOI: 10.1038/s41467-017-00427-5.
10. J. Nagamatsu, N. Nakagawa, T. Muranaka, Y. Zenitani, and J. Akimitsu, Nature, 2001; 410: 63.
11. Takaaki Koyanagi, Yutai Katoh, Caen Ang, Derek King, Greg E. Hilmas, William G. Fahrenholtz, Jr. American Chem. Soc., 2019; 102(1): 85.
12. Vlastimil Mazánek, Hindia Nahdi, Jan Luxa, Zdeněk Sofer and Martin Pumera, Nanoscale, 2018; 10: 11544.

13. H. Rosner, W. E. Pickett, S.-L. Drechsler, A. Handstein, G. Behr, G. Fuchs, K. Nenkov, K.-H. Muller, and H. Eschrig, Phys. Rev., 2001; B64: 144516.
14. A. Yamamoto, C. Takao, T. Masui, M. Izumi, and S. Tajima, Physica, 2002; C383: 197.
15. Z.-A. Ren, S. Kuroiwa, Y. Tomita, and J. Akimitsu, Physica, 2008; C468: 411.
16. A. Gauzzi, S. Takashima, N. Takeshita, C. Terakura, H. Takagi, N. Emery, C. Hérold, P. Lagrange, and G. Loupias, Phys. Rev. Lett., 2007; 98: 067002.
17. A. N. Kolmogorov and S. Curtarolo, Phys. Rev., 2006; B73: 180501R.
18. P. Zhang, S. Saito, S. G. Louie, and M. L. Cohen, Phys. Rev., 2008; B77: 052501.
19. D M Gaitonde, P Modak, R S Rao and B K Godwal, Bull. Mater. Sci., 2003; 26: 137.
20. S. Mollah, H. D. Yang, B. K. Choudhary, Ind. J. Phys., 2003; 77: 9.
21. Aleksey N. Kolmogorov, Matteo Calandra and Stefano Curtarolo, Phys. Rev., 2008; B78: 094520.
22. L. Kleinmann, Phys. Rev., 1967; 160: 585.
23. L. Kleinmann, Phys. Rev., 1968; 172: 385.
24. D. C. Langreth, Phys. Rev., 1969; 181: 753.
25. J. Hubbard, Proc. Roy. Soc. (London), 1957; A240: 539.
26. J. Hubbard, Proc. Roy. Soc. (London), 1957; A243: 356.
27. L. J. Sham, Proc. Roy. Soc. (London), 1965; A283: 33.
28. L. Kleinmann, Phys. Rev., 1967; 160: 585.
29. L. Kleinmann, Phys. Rev., 1968; 172: 385.
30. D. C. Langreth, Phys. Rev., 1969; 181: 753.
31. R. W. Shaw, J. Phys. C, 1970; 3: 1140.
32. K. S. Singwi, M. P. Toshi, R. H. Land and A. Sjolander, Phys. Rev., 1968; 176: 589.
33. K. Singwi, M. P. Toshi, A. Sjolander and R. H. Land, Phys. Rev., 1970; B1: 1044.
34. H. Khan and K. S. Sharma, IJPAP, 1998; 36: 523.
35. S. Sharma, H. Khan and K. S. Sharma, IJPAP, 2003; 41: 301.
36. W. L. Mc Millan, Phys. Rev., 1968; 167: 313.
37. P. P. Singh, Bull. Mat. Sc., 2003; 26: 131.
38. U. Burkhardt, V. Gurin, F. Hearmann, H. Borrmann, W. Schnelle, A. Yaresko, Y. Grin, Journal of Solid State Chemistry, 2004; 177(2): 389.